

# EXPERIMENTAL AND NUMERICAL STUDY OF VALVES FOR SUPERCRITICAL CARBON DIOXIDE BRAYTON CYCLE

**Haomin Yuan, Mark Anderson**  
Department of Engineering Physics  
University of Wisconsin-Madison  
1500 Engineering Drive, Madison, WI, 53706  
hyuan8@wisc.edu

## ABSTRACT

Supercritical Carbon Dioxide (sCO<sub>2</sub>) is a promising working fluid for future generation power cycles. The sCO<sub>2</sub> Brayton cycle shows advantages like high efficiency, compact, and low capital cost. In order to study this cycle, the valve characteristics under sCO<sub>2</sub> flow conditions must be understood. Due to the unique properties of sCO<sub>2</sub>, traditional models for valves may not be accurate. In this research, this problem is studied both experimentally and numerically. A relative small valve was tested in our experiment facility to provide validation data. Numerical predictions are very close to experiment data for the tested valve. Then the results are scaled up in simulation to the valves that are used in a designed power cycle. Traditional gas service valve model fails to predict mass flow rate for low pressure ratio. Modification is proposed to improve current gas service valve model.

## Keywords

Supercritical Carbon Dioxide, valve, OpenFOAM, Homogeneous Equilibrium Model

## 1. INTRODUCTION

In recent development of advanced high efficiency power cycles, supercritical fluid has been considered as a competitive candidate for working fluid. The increased operating temperature and pressure result in a significant increase of thermal efficiency. Among all designs of supercritical fluid power cycle, the Supercritical Carbon Dioxide (sCO<sub>2</sub>) Brayton cycle in its recompression version shows the optimal performance [1], [2]. This is due to the fact that sCO<sub>2</sub> Brayton cycle reaches a high efficiency with relative low operating temperature and pressure but remains simplicity. A lot of works have been conducted to perform optimization for sCO<sub>2</sub> Brayton cycle. Different designs have been proposed based on steady state analysis. Research based on transient off-design analysis is in great demand, which requires a study of control scheme.

In Dostal's discussion [1], three types of control schemes are adopted for sCO<sub>2</sub> Brayton Cycle. They are bypass control, inventory control, and temperature control. In bypass control the power output is controlled by regulating the mass flow rate through each component. Inventory control uses one or several inventory tanks to control the mass of sCO<sub>2</sub> in the cycle. Temperature control changes the turbine inlet temperature to control the cycle, by regulating the power level of coupled heat source. In bypass and inventory control, valves are the tools to change the cycle flow path. In bypass control, valves are placed to bypass the major components, such as turbine, recuperator, and cooler. In inventory control, inventory tanks extract or add inventory into the cycle through inventory inlet or outlet valves. As a result, it is important to know the valve characteristics with sCO<sub>2</sub> fluid. In this research, design by Moiseyev and Sienicki [3] is used to demonstrate a real design of control scheme in order to help valve selection. There are five valves in the main cycle of Moiseyev's design, as shown in Fig. 1. They are Turbine Bypass Valve (TBPv), Recuperator Bypass Valve (RBPv), Cooler Bypass Valve (CBPv), Inventory tank Inlet

Valve (INViv), and Inventory tank Outlet Valve (INVOv). As we can see from their names, TBPv, RBPv, and CBPv are for bypass control, and INViv and INVOv are for inventory control.

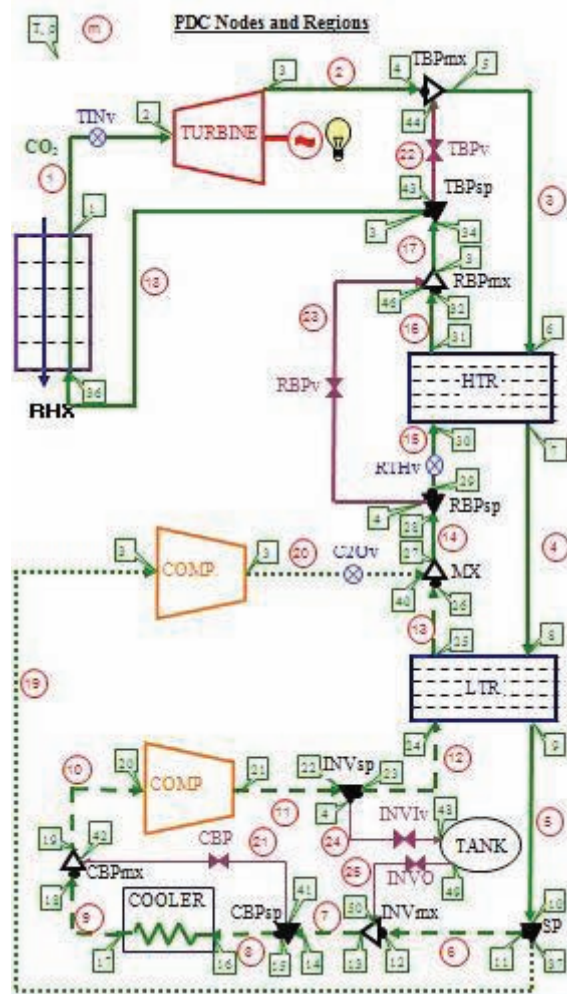


**Figure 1. sCO<sub>2</sub> Brayton Cycle by Moisseytsev [3]**

In order select proper valves, it is important to determine valve type and size. For better controlling purpose, globe valves are proposed to be used for all purposes. The remaining issue is to determine the size of valves. The ideal situation is for valve to utilize the full range of the stroke while producing the desired flow characteristics and maximum flow output. However, valves are rarely undersized because of the number of safety factors built into the user's service conditions and the manufacturer's sizing criteria. Because of these safety factors, a large number of valves actually end up being oversized. Although not ideal, an oversized valve is still workable. The valve coefficient ( $C_v$ ) is used to determine valve size [4]. As specified by the Instrument Society of America, the simplified equation of  $C_v$  is [4]

$$C_v = Q \sqrt{\frac{S_g}{\Delta P}} \quad (1)$$

where  $C_v$  = required valve coefficient for the valve  
 $Q$  = flow rate (in gal/min)  
 $S_g$  = specific gravity of the fluid relative to water (1000 kg/m<sup>3</sup>)  
 $\Delta P$  = pressure drop (psi)

However, the above correlation can only be used to determine the valve coefficient with incompressible fluid. To determine the valve coefficient for gas service, or use a manufacturer's provided valve coefficient to calculate mass flow rate, a modified equation is needed as shown in Eq. 2.

$$w = 63.3 F_p C_v Y \sqrt{x P_1 \gamma_1} \quad (2)$$

where  $w$  = gas flow rate (lb/h)  
 $F_p$  = piping-geometry factor  
 $C_v$  = valve coefficient  
 $Y$  = expansion factor,  $1 - x/(3x_T F_k)$   
 $x$  = pressure drop ratio,  $(P_1 - P_2)/P_1$   
 $P_1$  = upstream absolute pressure (psia)  
 $P_2$  = downstream absolute pressure (psia)  
 $\gamma_1$  = specific weight at inlet service condition (lb/ft<sup>3</sup>)  
 $F_k$  = ratio of specific heat transfer,  $k/1.40$   
 $k$  = ratio of specific heat of working fluid  
 $x_T$  = terminal pressure drop ratio

In order to properly apply Eq.2, a choked flow check is needed. When  $x < x_T F_k$ , the flow is not choked, and the value of  $x$  is used in calculation. When  $x > x_T F_k$ , the flow is choked, and  $x = x_T F_k$  in calculation. A more detailed discussion of the application of this equation can be found in Skousen [4]. It is proposed to improve the existing gas serve valve model by changing the method for choked flow check. The traditional method use empirical coefficient or specific experiment data using air, which is not applicable to sCO<sub>2</sub> conditions. The proposed modification is to use the isentropic discharge model to for choked flow check. A detailed description of the isentropic discharge model for sCO<sub>2</sub> can be found in Yuan[5].

## 2. TEST FACILITY

The test facility that provide experimental data is logically depicted in Fig. 2. A description of the conditions typically viewed at various points during a standard experiment can be seen in Fig. 3. This figure shows a temperature-entropy diagram with points labeled with respect to Fig. 2. More detail about this test facility, can be found in our previous research [6]–[8].

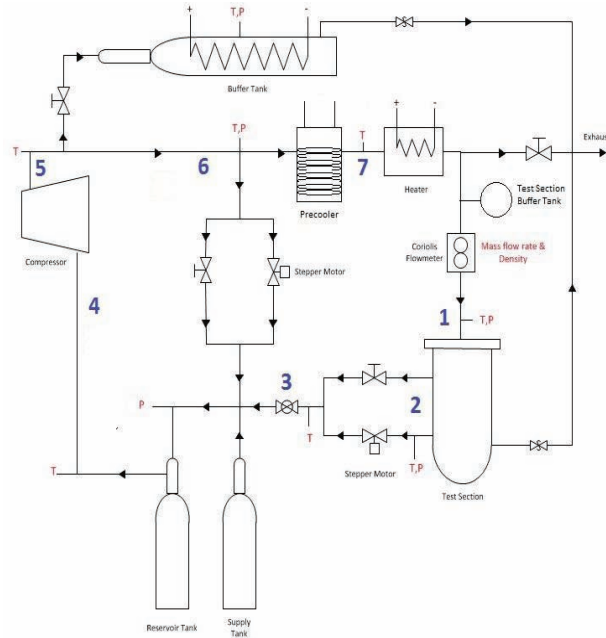


**Figure 2. Schematic diagram of sCO<sub>2</sub> test facility at UW-Madison**

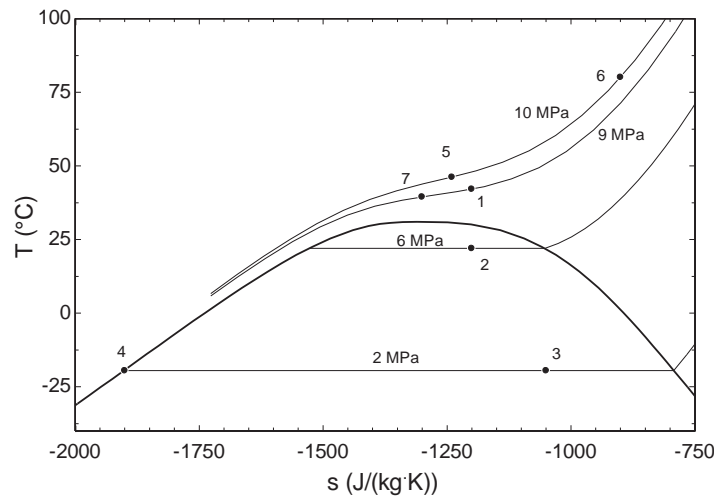


**Figure 3. T-s diagram of sCO<sub>2</sub> test facility at UW-Madison**

According to Edlebeck [7], the uncertainties from pressure, density, and mass flow rate measurements are presented in Table I. As we can see, the total uncertainties from each variables are significantly smaller than their values.

**Table I. Measurement uncertainties for experiment facility**

Measurement	Instrument	Resistance	Resolution	Total
Inlet pressure	17.24 kPa (2.50 psia)	5.61 kPa (0.814 psia)	1.30 kPa (0.19 psia)	18.18 kPa (2.63 psia)
Outlet pressure	17.24 kPa (2.50 psia)	5.62 kPa (0.816 psia)	1.30 kPa (0.19 psia)	18.18 kPa (2.63 psia)
Inlet density	1.0 kg/m <sup>3</sup>	0.325 kg/m <sup>3</sup>	0.076 kg/m <sup>3</sup>	1.05 kg/m <sup>3</sup>
Mass flow rate	1.0e-4 kg/s	3.3e-5 kg/s	7.6e-6 kg/s	1.06e-4 kg/s

The Metering Valve SS-31RS4 made by Swagelok [9] is tested in this facility to provide validation data. This valve has an orifice diameter of 0.064 in, which leads to a nominal maximum valve coefficient of 0.04. The valve's dimensions and inner geometry are presented in Fig. 4. This valve is connected to the inlet of the test section tank as show in Fig. 5. The subassembly is taken out of the tank, leaving it serves as a buffer tank to help maintaining stable downstream conditions.

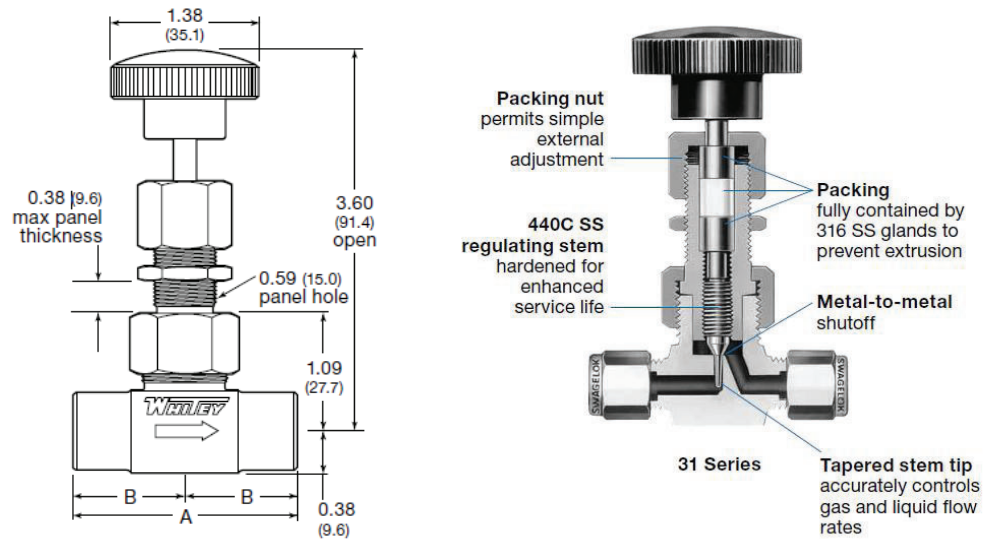


Figure 4. Dimensions and inner geometry of SS-31RS4[9]



Figure 5. Test valve connected to test loop

### 3. NUMERICAL METHODOLOGY

The numerical methodology is introduced with great detail in our previous papers [5], [10], [11]. Therefore, it is only briefly discussed in this section. The valves in sCO<sub>2</sub> Brayton Cycle are operating under varies conditions. As a result, the proposed numerical methodology should be able to handle all flow situation for sCO<sub>2</sub>, even for the possible appearance of two-phase. The open source CFD code OpenFOAM [12] is used for this research. Equation 3-5 represent the basic equations solved.

Continuity equation:

$$\nabla \cdot (\rho \cdot U) = 0 \quad (3)$$

Momentum equation:

$$\nabla \cdot (\rho \cdot U \cdot U) - \nabla \cdot (\mu_{effective} \cdot \nabla U) = -\nabla P \quad (4)$$

Energy equation:

$$\nabla \cdot (\rho \cdot U \cdot h) + \nabla \cdot (\rho \cdot U \cdot \frac{U^2}{2}) - \nabla \cdot (\rho \cdot \alpha_{effective} \cdot \nabla h) = 0 \quad (5)$$

Properties of sCO<sub>2</sub> are not internally implemented in the code of OpenFOAM. Therefore sCO<sub>2</sub> properties should be provided from an external module. REFPROP [13] was initially used. However, it was found that the use of REFPROP causes simulations to run extremely slowly. Properties of sCO<sub>2</sub> are currently provided by the FIT software library published by Northland Numerics [14], which provides an interpolated representation of properties. But the underlying property data are still obtained from REFPROP. In this way the FIT code calculates fluid properties much faster than REFPROP with acceptable error. A comparison of REFPROP and FIT can be found in [5].

Two-phase scenario should be handled as valves are operating in varies positions in the cycle. For simplicity, the Homogeneous Equilibrium Model (HEM) was chosen to model two-phase flow. It turns out HEM works very well for this problem, as we only concern about the prediction of mass flow rate. Turbulence is modeled by the standard k-ε model. More discussion about two-phase and turbulence modeling can be found in [5].

Fig. 6 illustrates the computational domain for the valve in Fig. 4. In order to save computational time, an axisymmetric geometry is used. The simulation geometry mimic the behavior of valve plug and seat. The meshing quality discussion can be found in our previous research for a similar flow condition of orifices [5].

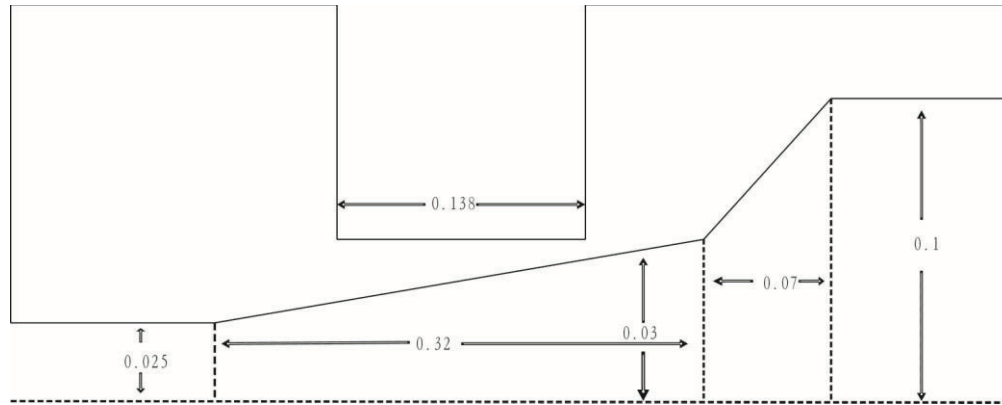


Figure 6. Computational domain for test valve geometry

#### 4. VALIDATION AND GAS SERIVE VALVE MODEL

In this section, the proposed numerical methodology is validated with experiment data first. Fig. 7 illustrates the mass flow rate through the tested valve predicted by simulation, comparing with experiment value at the same condition. Different open percentages are tested at a same upstream condition of 7.7 MPa at  $498 \text{ kg/m}^3$ . As we can see in Fig. 7, numerical predictions of mass flow rate are very close to experiment measurements. Other upstream conditions have also been tested, and the identical agreement is observed. The presented results are consistent with our previous research of orifice and labyrinth seal [5], [11]. The proposed numerical methodology shows a wide applicability for different geometries and conditions with  $\text{sCO}_2$ .

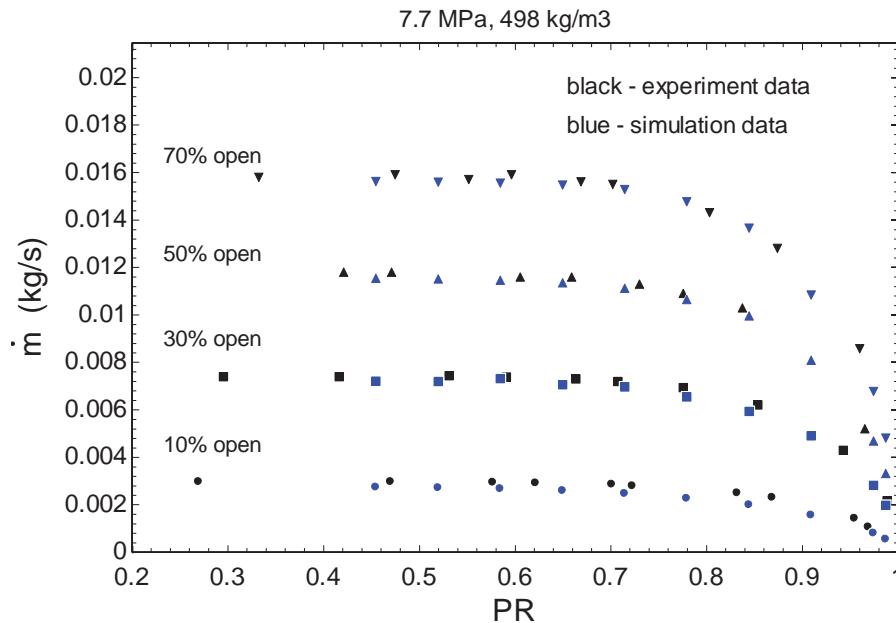


Figure 7. Comparison of experiment and simulation for test valve



In the rest of this part, the proposed modification of gas service valve model is examined by experiment and simulation data to demonstrate its improvement. The valve at 50% open is used as an example. Fig. 8 shows the valve coefficient changes with number of turns provided by manufacturer. For 50% open, which is 5 turns in Fig. 8, the valve coefficient is around 0.015. However, from both experiment and simulation, the valve coefficient at this opening is 0.02 at low pressure drop. Fig. 9 demonstrates the mass flow rate results from experiment, simulation, and model. As can be seen, using the valve coefficient of 0.015 underestimate the mass flow at high pressure ratio, and using the value of 0.02 overestimate the mass flow rate at low pressure ratio for the gas service model in Eq. 2. Fig. 9 also presented the results from the modified gas service valve model. The modified model with valve coefficient of 0.02 matches experiment data best.

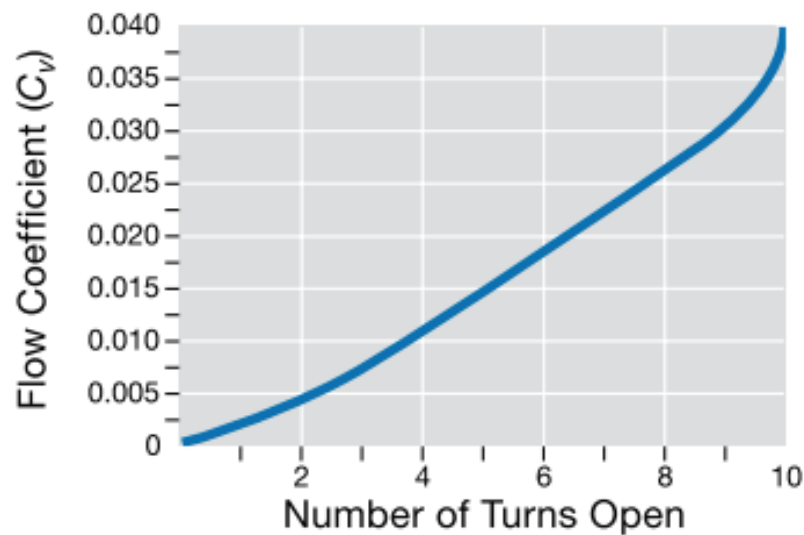


Figure 8. Valve coefficient changes with number of turns for tested valve

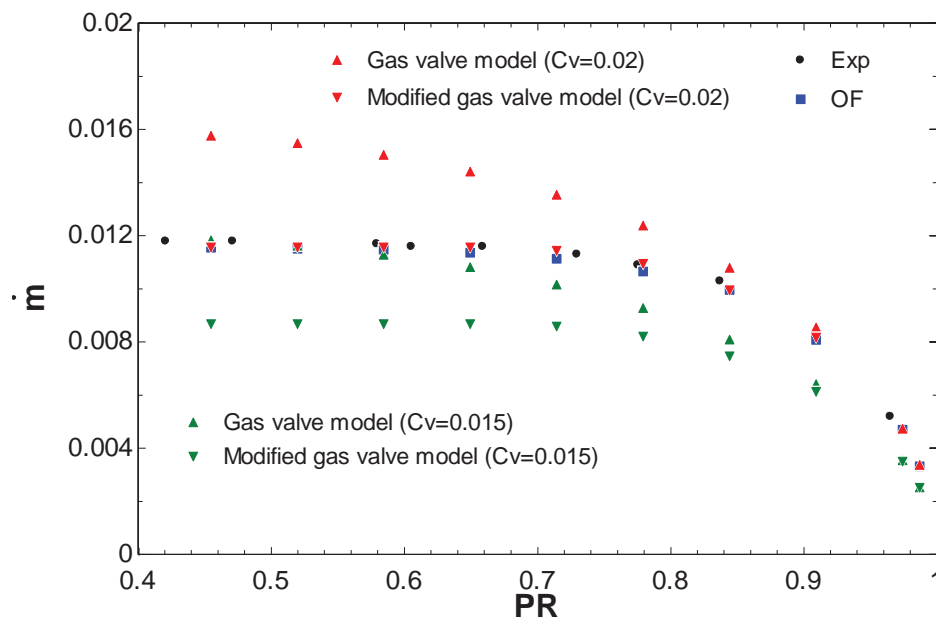


Figure 9. Mass flow rate of valve from different sources at 50% open



## 5. VALVE SELECTION AND GAS SERVICE VALVE MODEL

Two transients calculated by Moisseytsev [3] are used to help valve selection. One transient is for a shutdown process, the other is a down-up process. These transient data provide the upstream and downstream conditions of each valve, as well as the mass flow rate through them. The valve coefficients can be calculated at each time step, thus providing their maximum values presented in Table II. The corresponding upstream and downstream conditions at their maximum valve coefficient are presented as well.

In Table II, valves are significantly different in their requirements. The valves for bypass control, such as TBPv, RBPv, and CBPv, require large valve coefficients. These valves usually have a large amount of flow passing through them when operating. When they reach maximum valve coefficient, they have relative small pressure drops, which lead to small property difference across valves. This means traditional method is working for these valves, and nominal value provided by manufacturer is sufficient to help valve selection. However, the valves for inventory control, such as INVIV and INVOv, only need small valve coefficients. And the pressure drops across them is relative large at their maximum valve coefficient. Which means property difference across these valves are large, and sCO<sub>2</sub> property change should be considered. In the following part of this section, we focus on valve selection of INVIV and INVOv.

**Table II. Max valve coefficients**

Condition at max Cv	TBPv	RBPv	CBPv	INVIV	INVOv
$C_{v_{max}}$	7489.99	14818.44	5552.48	29.13	25.74
$P_{inlet}$ (Pa)	7.67E+06	1.60E+07	7.68E+06	1.50E+07	8.52E+06
$P_{outlet}$ (Pa)	7.58E+06	1.59E+07	7.66E+06	1.40E+07	7.61E+06
$T_{inlet}$ (C)	327.81	210.11	85.26	87.75	42.27
$T_{outlet}$ (C)	347.33	339.92	33.00	70.30	89.08
$\rho_{inlet}$ (kg/m <sup>3</sup> )	68.65	195.94	146.31	382.90	313.71
$\rho_{outlet}$ (kg/m <sup>3</sup> )	65.46	140.15	381.09	452.24	141.31
$\dot{m}$ (kg/s)	438.15	703.05	231.39	13.98	10.41

The nuclear application valves report from Flowserve [15] helps us to select proper valves. According to the pressure and temperature range of sCO<sub>2</sub> Brayton cycle, all valves should be in Class 1500. Parameters of Class 1500 globe valve are presented in Table III to help select proper valves. In Table III, the valve with 2.5 in Nominal Pipe Size (NPS) can provide the valve coefficient needed by INVIV and INVOv. However, the parameters in Table III are obtained from traditional tests using water and air. It is necessary to perform experimental or numerical test for this valve under sCO<sub>2</sub> condition. However, our test facility cannot provide the mass flow rate for a valve with 2.5 in NPS. As a consequence, the numerical approach introduced previously is used. The valve's seat and plug geometries are presented in Fig. 10 for the globe valve by Flowserve. There are three types of plug, Standard, Cage, and Parabolic. For better control purpose, the Parabolic plug should be selected. Fig. 11 shows the computational domain for this globe

valve with a Parabolic plug of 50% open. However, the dimensions in Fig. 11 are scaled from graphics in [15], not from a real valve.

**Table III. Class 1500 globe valve's maximum valve coefficient by Flowserve [15]**

NPS (in)	2.5	3	4	6	8
Max Cv	83.3	119	201	435	733

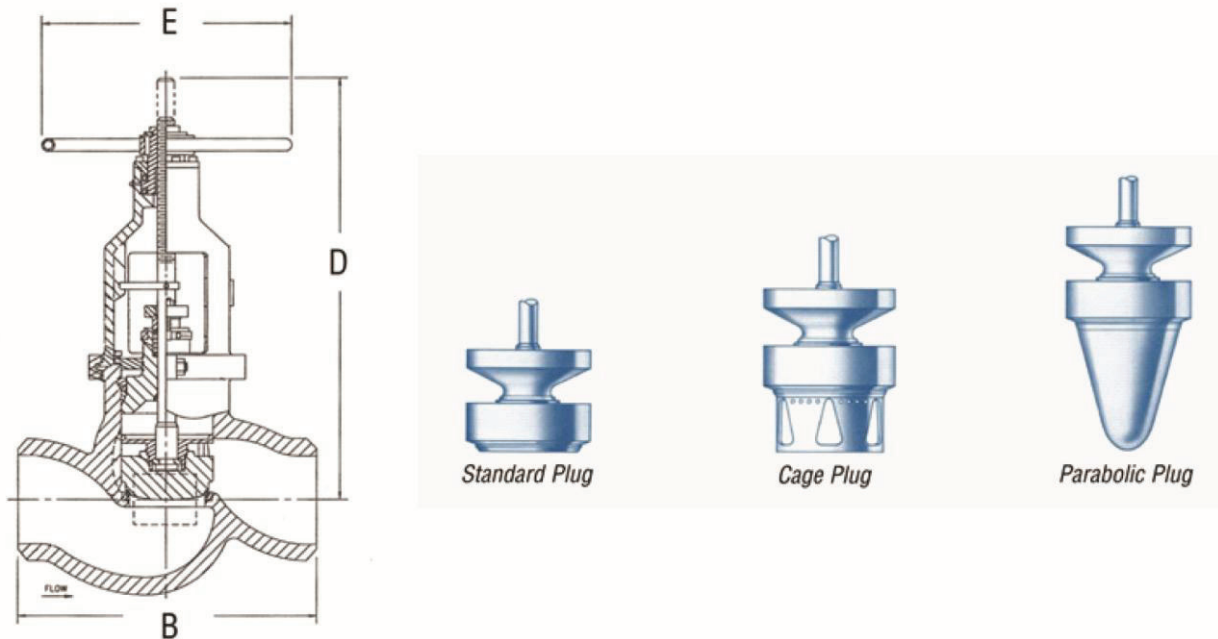


**Figure 10. Globe valve and plugs by Flowserve[15]**

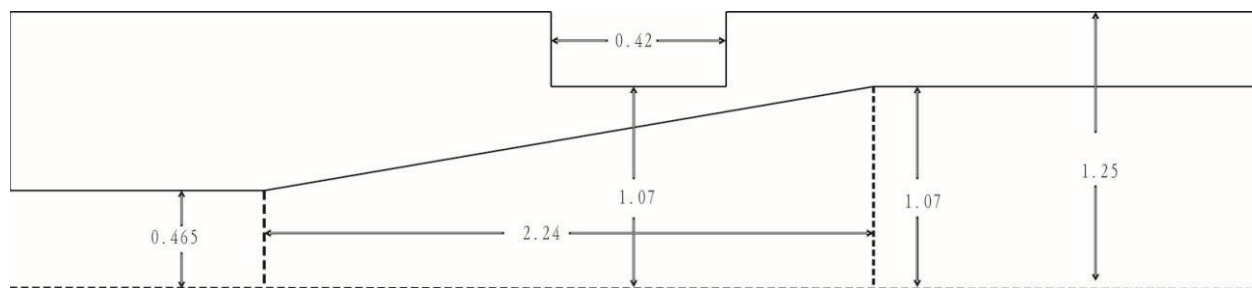


**Figure 11. Computational domain for globe valve by Flowserve**

In the following part, three different upstream conditions were tested (shown in Fig. 12) for the geometry in Fig.11. However only one of them is presented here. Fig. 13 presents the data with upstream condition of 7.7 MPa at 498 kg/m<sup>3</sup>. This valve at this open percentage has a valve coefficient of 60 which is obtained from simulation data at low pressure drop. When using this valve coefficient, the modified gas

valve model can provide a very good prediction of mass flow rate. Data from other upstream conditions show the similar result.

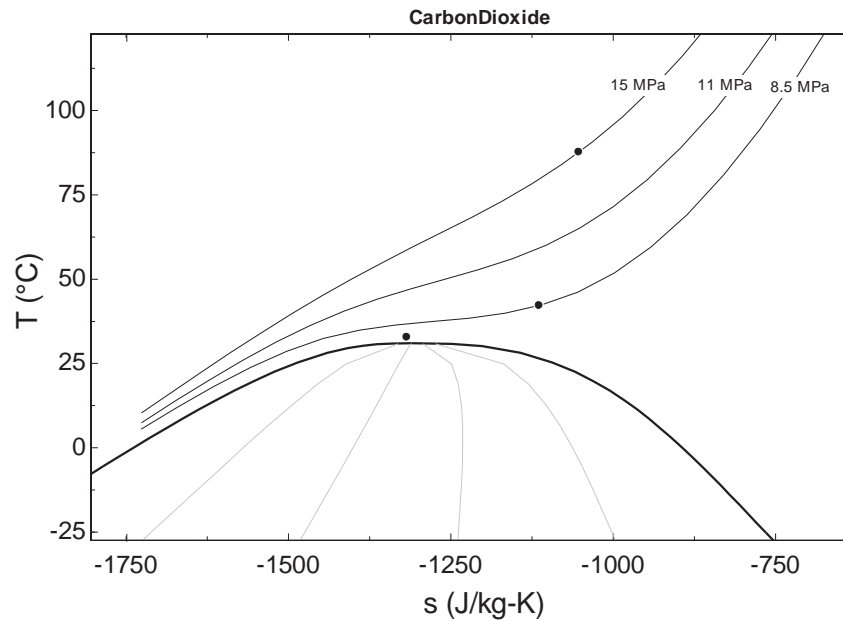


**Figure 12. Tested upstream conditions**

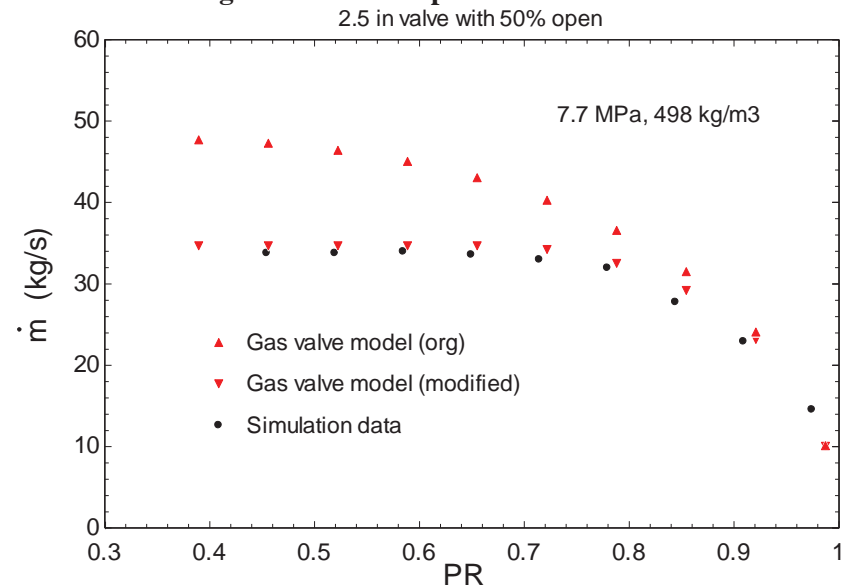


**Figure 13. Globe valve with 50% open with upstream condition of 7.7 MPa at 498 kg/m<sup>3</sup>**

## 6. MACH NUMBER AND CAVITATION

After valves are selected, the Mach number and cavitation should be inspected. This can only be achieved by examine the simulation data. Fig. 14 and 15 show the Mach number distribution for the simulated 2.5 in NPS valve at the conditions in Table II for INVIv and INVOv. The sound speed in two-phase region is defined in Eqn.6.

$$c^2 = \left. \frac{\partial P}{\partial \rho} \right|_s \quad (6)$$

where  $c$  is sound speed (m/s),  $P$  is pressure (Pa),  $\rho$  is density defined from HEM (kg/m<sup>3</sup>),  $s$  is specific entropy (J/kg·K).

As the maximum Mach numbers are less than one for both cases, it is fine to use this valve. For the conditions represented in Fig. 14 and 15, two-phase scenario does not show up. However, if further reducing the downstream pressure, two-phase may appear. However as two-phase flow is modeled by HEM, the cavitation cannot be presented precisely with the visualization of bubble formation and collapse. Therefore, a very qualitative representation of cavitation is presented. Fig. 16 and 17 present the quality distribution for reduced downstream pressures at the upstream conditions in Fig. 14 and 15. Even though downstream conditions are above saturation line, cavitation still appears. Therefore, special designs or materials should be considered at the locations of cavitation.

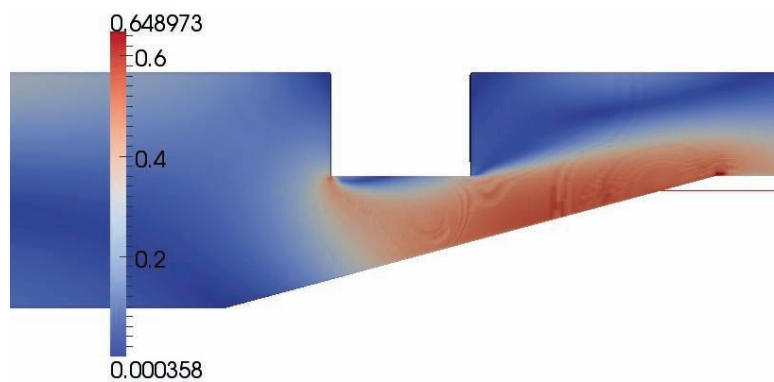


**Figure 14. Mach number of upstream of 8.5 MPa at 313 kg/m<sup>3</sup>, and downstream of 7.6 MPa**

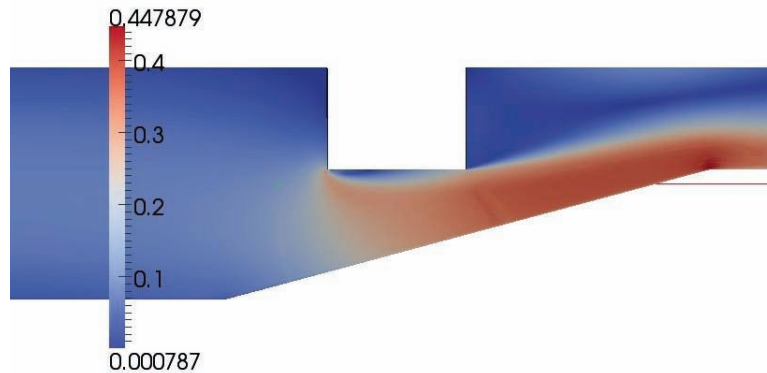


**Figure 15. Mach number of upstream of 15 MPa at 383 kg/m<sup>3</sup>, and downstream of 14 MPa**

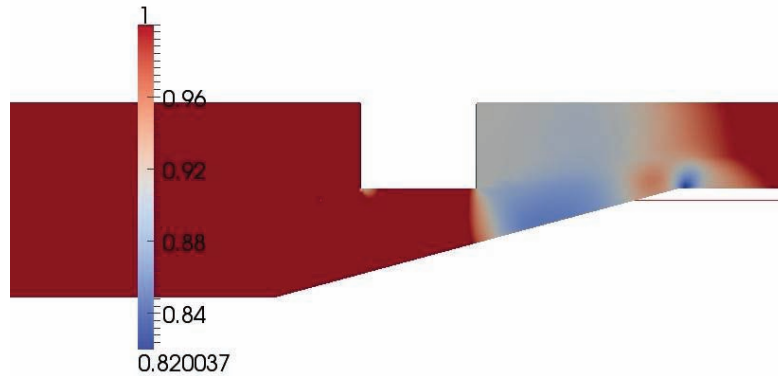


**Figure 16. Quality of upstream of 8.5 MPa at 313 kg/m<sup>3</sup>, and downstream of 7.0 MPa**

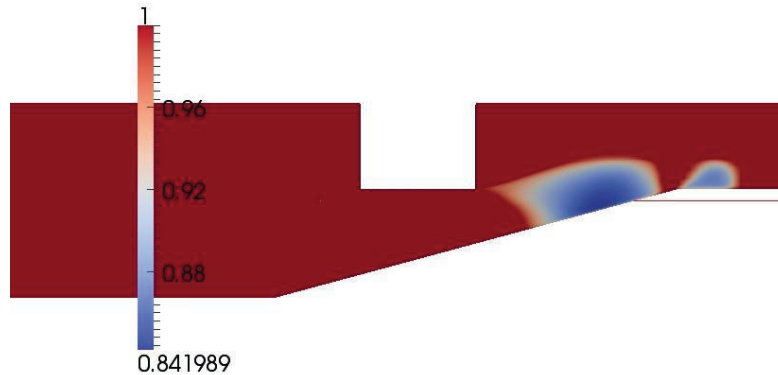


**Figure 17. Quality of upstream of 15 MPa at 383 kg/m<sup>3</sup>, and downstream of 9.0 MPa**

## 7. CONCLUSION

Valve characteristics for sCO<sub>2</sub> are studied with both numerical and experimental approaches. The numerical method is validated with experiment data obtained from a small-scale valve for different conditions. The traditional gas service valve model is examined with limitation pointed out of choked flow check method. It is proposed to use the isentropic discharge model choking point to check choked flow. The requirements for each valve in a sCO<sub>2</sub> Brayton cycle from two transients are used to select the proper size for them. This paper provides an example to use the proposed numerical methodology to help valve selection for sCO<sub>2</sub> Brayton cycle. Meanwhile, the modified gas valve model shows a great improvement compare with traditional model. In this study, only the valves for cycle control purpose are studied. Valves for other purposes, such as pressure relief, could be studied using the same method.

## ACKNOWLEDGMENTS

The authors would like to thank Dr Moisseytsev from Argonne National Laboratory for providing data for valve selection and making valuable suggestions for this research.

## REFERENCES

1. V. Dostal, "A Supercritical Carbon Dioxide Cycle for Next Generation Nuclear Reactors," Doctoral dissertation, Massachusetts Institute of Technology, 2004.
2. V. Dostal, P. Hejzlar, and M. J. Driscoll, "The Supercritical Carbon Dioxide Power Cycle : Comparison to Other Advanced Power Cycles," *Nuclear technology*, vol. 154, no. 1, pp. 283–301, 2006.
3. A. Moiseyev and J. Sienicki, "Development of a Plant Dynamics Computer Code for Analysis of a Supercritical Carbon Dioxide Brayton Cycle Energy Converter Coupled to a Natural Circulation Lead-Cooled Fast Reactor," Chicago, IL, USA, 2006.
4. P. L. Skousen, *VALVE HANDBOOK*. McGraw-Hill, 1998.
5. H. Yuan, J. Edlebeck, M. Wolf, M. Anderson, M. Corradini, S. Klein, and G. Nellis, "Simulation of Supercritical CO<sub>2</sub> Flow through Circular and Annular Orifice," *Journal of Nuclear Engineering and Radiation Science*, 2014.
6. M. A. Rodarte, "The Development of an Experimental Test Facility to Measure Leakage through Labyrinth Seals," Master Thesis, University of Wisconsin-Madison, 2011.
7. J. P. Edlebeck, "Measurements And Modeling of The Flow of Supercritical Carbon Dioxide," Master Thesis, University of Wisconsin-madison, 2013.
8. M. P. Wolf, "Flow of Supercritical Carbon Dioxide Through Annuli And Labyrinth Seals," Master Thesis, University of Wisconsin-madison, 2014.
9. "Metering Valves." [Online]. Available: <http://www.swagelok.com/downloads/webcatalogs/En/MS-01-142.pdf>.
10. H. Yuan, M. H. Anderson, J. Dyreby, J. Edlebeck, and M. Wolf, "Simulations of the Flow of Supercritical Carbon Dioxide through Circular and Annular Orifices," in *Transaction of the American Nuclear Society*, 2013, vol. 109, pp. 301–303.
11. H. Yuan, S. Pidaparti, M. Wolf, and M. Anderson, "Experiment And Numerical Study of Supercritical Carbon Dioxide Flow Through Labyrinth Seals," in *The 4th International Symposium on Supercritical CO<sub>2</sub> Power Cycles*, 2014.
12. OpenCFD Limited, "OpenFOAM User Guide," 2011. [Online]. Available: <http://www.openfoam.org/docs/user/>.
13. E. W. Lemmon, M. L. Huber, and M. O. McLinden, "NIST Reference Fluid Thermodynamic and Transport Properties-REFPROP," Boulder, Colorado, 2007.
14. Northland Numerics, "FIT," 2012. [Online]. Available: <http://www.northlandnumerics.com/>.
15. "Edward and Anchor/Darling Nuclear Application Valves." [Online]. Available: <http://www.flowserve.com/files/Files/Literature/ProductLiterature/FlowControl/AnchorDarling/EVENCT0004-01.pdf>.